

First-principles calculations of quantum paraelectric $\text{La}_{1/2}\text{Na}_{1/2}\text{TiO}_3$ in the virtual-crystal approximation: Structural and dynamical properties

Grégory Geneste,^{1,*} Jean-Michel Kiat,^{1,2} and Charlotte Malibert¹

¹Laboratoire Structures, Propriétés et Modélisation des Solides, CNRS-UMR 8580, Ecole Centrale Paris, Grande Voie des Vignes, 92295 Chatenay-Malabry Cedex, France

²Laboratoire Léon Brillouin, CE Saclay CNRS-UMR 12, 91991 Gif-sur-Yvette Cedex, France

(Received 1 June 2007; revised manuscript received 18 November 2007; published 29 February 2008)

The virtual crystal approximation is applied to $\text{La}_{1/2}\text{Na}_{1/2}\text{TiO}_3$ (LNTO) to account for the chemical disorder. The structural distortions (tilt angles, interatomic bondlengths) are reproduced with a very good accuracy. Linear response calculations within this approximation predict that this compound has very weak ferroelectric instabilities (weaker than in SrTiO_3) along two directions of the orthorhombic structure, which suggests that LNTO is a quantum paraelectric. The mechanisms responsible for the low-temperature dielectric behavior of LNTO are in nature different from those in CaTiO_3 . Our calculations also predict a strong anisotropy in the dielectric response of this compound.

DOI: 10.1103/PhysRevB.77.052106

PACS number(s): 61.50.Ah, 77.84.-s, 71.15.Mb

The understanding and simulation of the effect of the chemical disorder in solids is probably one of the most difficult topics of modern solid state physics. A simple and intuitive way to proceed in the theoretical treatment of the disorder is to use as large as possible supercells with periodic boundary conditions. Unfortunately this approach is not compatible with first-principles calculations which require, even for supercells containing a few tens of atoms, a large amount of computational time and power.

An alternative approach is to use the so-called “virtual crystal approximation” (VCA). In density-functional calculations using pseudopotentials, this approach is based on the creation of a virtual chemical element that mixes the pseudopotentials of the elements involved in the chemical disorder. This average can be achieved according various schemes. In the most simple one, for an alloy/solid solution A_xB_{1-x} in which A and B randomly occupy a given site or sublattice of a crystalline structure, one can replace A and B by a virtual element represented by a pseudopotential operator $\hat{V}_{ps} = x\hat{V}_{ps}^A + (1-x)\hat{V}_{ps}^B$. In this approach, the number of valence electrons to be accounted for is an average of the A and B valence electron numbers treated by each atomic pseudopotential \hat{V}_{ps}^A and \hat{V}_{ps}^B .

The VCA has been successfully applied to a number of materials, from semiconductor alloys to perovskite solid solutions such as PZT,^{1–4} BST,⁵ or PSN.^{6,7} It seems to work satisfactorily to a certain extent provided the mixed pseudopotentials have similarities. In this work we apply this particular approach to $\text{La}_{1/2}\text{Na}_{1/2}\text{TiO}_3$ (LNTO), a crystal which has recently attracted the interest due to its peculiar dielectric properties at low temperature. About fifteen years ago, LNTO was shown by Inaguma *et al.*⁸ to have a temperature-independent dielectric constant below ≈ 90 – 100 K. This saturation of ϵ_S to a quite high value (100–200) at low temperature was confirmed by other authors^{9–12} and suggested to be related to a “high-temperature” quantum paraelectric behavior since the saturation temperature T_S , as obtained from a fit within the Barrett relation, is much higher than the values found in standard quantum paraelectric crystals such as SrTiO_3 (STO) or KTaO_3 (KTO).

In a recent work,¹² we determined from neutron diffraction experiments the structure of LNTO unambiguously (space group $Pnma$ —Glazer notation: $a^-b^+a^-$). In this compound, the La and Na atoms randomly occupy the A site of the perovskite structure. From first-principles, we studied ordered supercells with various orders and structures. From frozen-phonon calculations of ferroelectric and antiferrodistortive instabilities, and from the optimization of tilted structures, the chemical disorder experimentally observed in this compound was suggested to decrease the structural distortions as well as the dielectric response. Our calculations suggested that ordered LNTO structures are quantum paraelectric systems. Interestingly, the ordered structure (space group $Pmn2_1$) was found to have a very anisotropic dielectric response, very large along y and about twice lower along z : at the LDA lattice parameters we had $\epsilon_{S,xx}=233$, $\epsilon_{S,yy}=321$, $\epsilon_{S,zz}=157$. At the experimental lattice constants, the TO mode responsible for the large response along y becomes unstable, suggesting a quantum paraelectric behavior in such structures as well as a strong anisotropy in the dielectric response.

In this paper, we employ VCA calculations to investigate the structure and dynamics of disordered LNTO. We show that the VCA describes very well the structure of this compound, and predicts the existence of weak ferroelectric (FE) instabilities in the $Pnma$ structure, along y and x . The axis are defined as in Ref. 12: in the Glazer equivalent notation for $Pnma$ group ($a^-b^+a^-$), this space group implies to take as new cell axis for the orthorhombic primitive cell, two axis x and z at 45° of the cubic cell and the latter y axis along the b -cubic axis, but with a doubled value.

The calculations are performed in the framework of the density functional theory (DFT)¹³ in the local density approximation (LDA).¹⁴ We use the ABINIT code,¹⁵ pseudopotentials of the Troullier-Martins type,¹⁶ and a plane-wave cut-off of 40 Ha. The first Brillouin zone (FBZ) is sampled with a k -point mesh corresponding to $6 \times 6 \times 6$ in the FBZ of the five-atom unit cell, for the self-consistent calculation of the total energy as well as for the calculation of the phonon bandstructure of the cubic structure. Structural optimizations

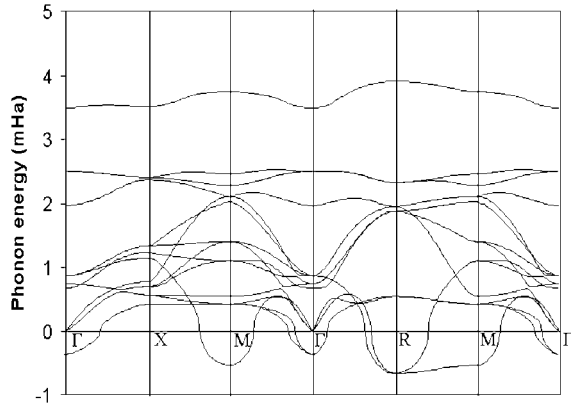


FIG. 1. Phonon bandstructure of LNTO within the VCA, computed at the theoretical lattice constant (3.87 Å).

are performed within a tolerance on maximal forces of 0.01 eV/Å. We use the virtual crystal approximation as implemented in the ABINIT code, to create a fictitious chemical element on the *A* site of the perovskite: the La and Na pseudopotential operators are mixed according to the corresponding atomic probabilities. The Na and La pseudopotentials, which are mixed, are generated from the ionic configuration that corresponds to their formal oxidation states (+I and +III respectively) in the perovskite structure. Semicore electrons are included in the calculations for La, Na, and Ti (see Ref. 12).

The ideal cubic structure (space group $Pm\bar{3}m$) is first optimized within the VCA: one obtains a (theoretical) lattice constant of 3.870 Å. It is noteworthy that this value is very close to the experimental (pseudocubic) lattice constant measured in LNTO: for instance, our group finds $a_p=3.872$ Å from neutron diffraction experiments at $T=1.5$ K.¹² The underestimation is very weak (0.05%), which is quite unusual with the LDA (typically, the underestimation of the lattice constant within this approximation is rather $\approx 1-2\%$). This may be due to the alchemical mixing of the La and Na pseudopotentials. To investigate the possible instabilities in LNTO, the phonon bandstructure is computed on the whole Brillouin zone at this theoretical lattice parameter (see Fig. 1). Unstable modes at *R* and *M* are expected and found (especially pronounced at *R*) since the ground state structure is known to be *Pnma* ($a^-b^+a^-$ in Glazer notation). We also note a polar instability at Γ , less strong than the antiferrodistortive instabilities at the *R* and *M* points.

The structure of LNTO in the *Pnma* space group is then optimized within the VCA. First the cell is completely optimized (atomic positions, cell size and shape until maximal components of the stress tensor is $\leq 2 \times 10^{-4}$ eV/Å³). One obtains $a=5.463$ Å, $b=7.708$ Å, $c=5.483$ Å. The corresponding pseudocubic parameter is $a_p=3.865$ Å. The geometric parameters (bondlengths, bond angles) corresponding to this fully optimized geometry are gathered in Table I.

Then we use the experimental lattice constants determined by our group from neutron diffraction experiments¹² and only optimize the atomic positions. The optimized interatomic distances and angles are given in Table I. They are

TABLE I. Comparison of structural data in LNTO from neutron refinements ($T=1.5$ K) and our LDA calculations in the [111]-ordered structure (Ref. 12) in the $Pmn2_1$ space group and in the virtual crystal approximation (space group *Pnma*), optimized at the experimental lattice constants (1) ($a=5.4749$ Å, $b=7.7374$ Å, $c=5.4820$ Å) and at the theoretical lattice constants (2) ($a=5.463$ Å, $b=7.708$ Å, $c=5.483$ Å).

Method	LNTO neutrons	ordered LNTO LDA	VCA	VCA
			LNTO (1)	LNTO (2)
space group	<i>Pnma</i>	$Pmn2_1$	<i>Pnma</i>	<i>Pnma</i>
Ti-O2 (Å)	1.947	1.894;1.911	1.948	1.948
	1.950	2.003;2.047	1.949	1.949
	2.738	2.722;2.781	2.739	2.736
O2-O2 (Å)	2.773	2.795;2.802	2.772	2.775
	La-O1 Na-O1			
	La/Na-O1 (Å)	2.484	2.475;2.395	2.489
	2.716	2.556;2.627	2.714	2.678
	2.783	2.971;2.881	2.793	2.817
	2.999	3.023;3.093	2.993	2.999
La-O2 Na-O2				
La/Na-O2 (Å)	2.577	2.456;2.506	2.555	2.529
	2.611	2.587;2.712	2.619	2.641
	2.864	2.759;2.732	2.839	2.787
	2.915	3.188;3.051	2.951	2.985
O1-O2 (Å)	2.730	2.740;2.768	2.751	2.749
	2.746	2.771;2.771	2.754	2.752
	2.768	2.778;2.792	2.765	2.756
	2.787	2.780;2.802	2.767	2.759
Ti-O1-Ti (°)	164.85	164.15;156.99	163.91	163.78
Ti-O2-Ti (°)	167.44	158.04;164.45	167.45	166.48
Θ (anti-phase) (°)	7.58	9.68	8.04	8.11
Φ (in-phase) (°)	0.91	9.21	1.84	3.29

compared to the experimental results¹² and the ones obtained in ordered structures of LNTO in the $Pmn2_1$ space group from first-principles. The notations employed to describe the *Pnma* structure (O1, O2) refer to Fig. 2 of Ref. 12.

The agreement between the low-temperature results and the VCA is very good: the interatomic bonds agree within at most 0.02 Å, and for the angles, the VCA provides Φ (in-phase angle)=1.84° (expt: 0.91°) and Θ (antiphase angle)=8.04° (experiment: 7.58°). The agreement between the VCA and the experiments for the in-phase angle is very good, as compared to the much larger angle obtained in the ordered structures ($\Phi=9.2^\circ$).

We now turn to linear response calculations, performed within the density functional perturbation theory (DFPT) as implemented in the ABINIT code. At Γ in the *Pnma* structure, we find *two* unstable polar modes with close imaginary eigenfrequencies 70i and 49i cm⁻¹ and irreducible representation B_{2u} and B_{3u} of point group D_{2h} . They correspond to very weak ferroelectric instabilities. In a classical treatment

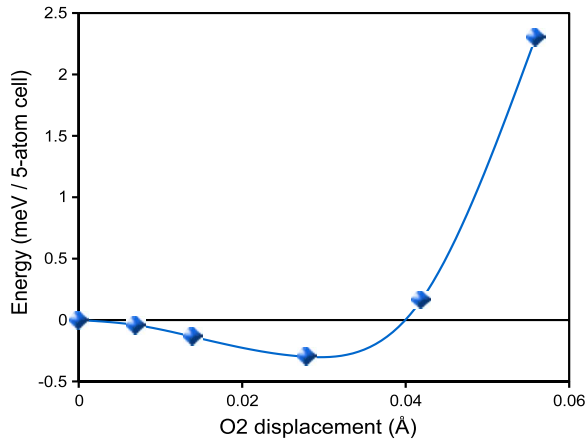


FIG. 2. (Color online) Total energy as a function of the FE distortion in LNTO, following the lowest-frequency mode at $70i$ cm^{-1} .

of the atomic motions, one would conclude that $Pnma$ is not the ground state structure of LNTO. Anyway, it is possible to compare the magnitude of these instabilities to the ones obtained in quantum paraelectric crystals (from a similar theoretical scheme): SrTiO_3 (STO), for example, also contains, in its tetragonal $I4/mcm$ low temperature paraelectric phase,¹⁸ unstable TO modes at $90i$ and $96i$ cm^{-1} . These imaginary eigenfrequencies are much higher in classical ferroelectric crystals, such as BaTiO_3 (BTO): in its paraelectric structure (cubic $Pm\bar{3}m$),¹⁷ BTO contains three unstable modes (TO1) at $219i$ cm^{-1} . It is well known that the FE instability of STO is suppressed by the quantum effects associated with the zero point motions.¹⁹ Thus we can infer that in LNTO, the FE instability, weaker than in STO, is also suppressed by such effects. Therefore the VCA suggests that LNTO is a quantum paraelectric according to the definition of Müller and Burckard.²⁰

Interestingly, no FE instability is found along the z direction. This is coherent with the result obtained in the ordered $Pmn2_1$ structure, in which, at the LDA lattice parameters, the dielectric response along z is much lower than along x and y .¹² The present calculation therefore predicts a strong anisotropy in the dielectric response of LNTO.

To estimate the magnitude of the polar instabilities, we now perform a frozen-phonon calculation of the lowest-frequency unstable TO mode ($70i$ cm^{-1}). Distorting the crystal along this TO mode lowers its total energy by less than 0.5 $\text{meV}/5\text{-atom cell}$ (see Fig. 2), a very weak stabilization regarding quantum paraelectric crystals such as STO (≈ -2.7 $\text{meV}/5\text{-atom cell}$ ¹⁸) or FE crystals such as BTO (≈ -30 $\text{meV}/5\text{-atom cell}$ along $\langle 111 \rangle$ ¹⁷). This clearly suggests that quantum fluctuations are able to suppress such a distortion and maintain the system in a nonpolar $Pnma$ geometry. The eigendisplacements of the two FE modes of LNTO, as obtained from the VCA, are represented on Fig. 3: they have mainly components on O and Ti atoms. Their amplitudes are given in Table II. The electronic dielectric tensor is close (slightly higher) to what is found in ordered structures, with $\epsilon_{xx}^\infty = 7.13$, $\epsilon_{yy}^\infty = 7.11$, and $\epsilon_{zz}^\infty = 7.28$, as well as the atomic Born effective charges (for the fictitious atom Na/La

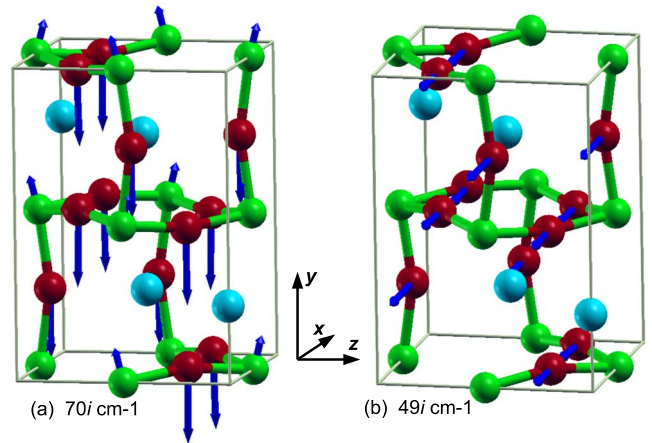


FIG. 3. (Color online) Eigendisplacements of the two FE modes ($70i$ and $49i$ cm^{-1}) of LNTO. Red: O, green: Ti, blue: La/Na. In the second case ($49i$ cm^{-1}), the Ti components of the eigendisplacement vector are not visible since they are along $+x$ and of smaller amplitude than the oxygen ones.

they are slightly higher than the mean value of La and Na, with $Z_{xx}^* = 2.90$, $Z_{yy}^* = 2.86$ and $Z_{zz}^* = 3.00$). The mode effective charges of the two previously described unstable modes are high (16.4 and 16.0 , respectively). Let us note that the lowest-frequency mode with B_{1u} symmetry (driving a polarization along z) is also highly polar (mode effective charge = 16.7) and very soft (42 cm^{-1}).

Let us compare LNTO to CTO: CTO was shown by Kim *et al.*²¹ to have a low-temperature behavior similar to LNTO: its dielectric constant saturates below ≈ 50 K to reach $\approx 300\text{--}400$ at $T=0$ K. Nevertheless, the dynamics of phonons has been investigated from first-principles DFT calculations in CTO by Cockayne and Burton,²² in the framework of the local density approximation. They showed that, according to this approximation, in its ground-state crystal structure (space group $Pnma$, as LNTO), CTO does not have unstable modes, suggesting that this compound is not a real quantum paraelectric crystal in the sense given by Müller and Burckard. The high value of ϵ_S is attributed in CTO to the existence of low-frequency (but stable) TO modes. For

TABLE II. Eigendisplacements of the two unstable modes found in the $Pnma$ space group at the theoretical lattice constants (10^{-3} atomic units).

Mode		x	y	z
$70i$ cm^{-1} (B_{2u})	La/Na	0.0	0.3	0.0
	Ti1	0.0	0.9	-0.2
	Ti2	0.0	0.9	0.2
	O1 (4c)	0.0	-1.3	0.0
	O2 (8d)	0.0	-1.4	0.0
$49i$ cm^{-1} (B_{3u})	La/Na	0.4	0.0	0.0
	Ti	0.7	0.0	0.0
	O1 (4c)	-1.6	0.0	0.0
	O2 (8d)	-1.3	0.0	0.0

this reason, we suggested in our previous work¹² that ordered LNTO is intermediate between CTO and STO. Our present LDA calculations suggest that disordered LNTO (i.e., the real LNTO compound) is a quantum paraelectric as well and is thus, in nature, different from CTO. In LNTO, according to the VCA, the high dielectric response at low temperature would be the result of unstable polar modes (FE instabilities), too weak anyway to provide structural distortions, which are suppressed by quantum zero-point motions.

Anyway the standard approximations of DFT may fail to describe correctly the weak instabilities in perovskites: for example, it has been shown that in KTO,^{23,24} no unstable polar mode are found by the calculations in the cubic structure, neither in the LDA nor in the GGA. And yet KTO is known to be an incipient ferroelectric, very similar to STO, with a very low saturation temperature. Akbarzadeh *et al.*²⁴

have shown that neither the LDA nor the GGA are able to reproduce the low-temperature dielectric behavior of KTO.

In this report, we have calculated from first-principles the structure and dynamical properties at Γ of LNTO, using the virtual crystal approximation within the LDA. We have found that the structure is quite nicely described. Two ferroelectric instabilities are found in the space group *Pnma*, along *x* and *y*, with very low imaginary eigenfrequencies, suggesting that LNTO is a quantum paraelectric and could have a very anisotropic dielectric response. Further experimental investigation is needed to improve the understanding of this compound.

Part of these calculations have been performed on the CNRS-IDRIS Supercomputing Center. Figure 3 has been obtained within the XCRYSDEN software (Ref. 25).

*gregory.geneste@ecp.fr

¹L. Bellaïche and David Vanderbilt, Phys. Rev. B **61**, 7877 (2000).

²L. Bellaïche, Alberto García, and David Vanderbilt, Phys. Rev. Lett. **84**, 5427 (2000).

³K. Leung, E. Cockayne, and A. F. Wright, Phys. Rev. B **65**, 214111 (2002).

⁴N. J. Ramer and A. M. Rappe, Phys. Rev. B **62**, R743 (2000).

⁵Ph. Ghosez, D. Desquesnes, X. Gonze, and K. M. Rabe, AIP Conf. Proc. **535**, 102 (2000).

⁶R. Haumont, A. Al-Barakaty, B. Dkhil, J.-M. Kiat, and L. Bellaïche, Phys. Rev. B **71**, 104106 (2005).

⁷R. Haumont, B. Dkhil, J.-M. Kiat, A. Al-Barakaty, H. Dammak, and L. Bellaïche, Phys. Rev. B **68**, 014114 (2003).

⁸Y. Inaguma, J.-H. Sohn, I.-S. Kim, M. Itoh, and T. Nakamura, J. Phys. Soc. Jpn. **61**, 3831 (1992).

⁹Sun, Pai-Hsuan, T. Nakamura, Y.-J. Shan, Y. Inaguma, and M. Itoh, Ferroelectrics **200**, 93 (1997).

¹⁰R.-M. Rao, H. Munekata, K. Shimada, M. Lippmaa, M. Kawasaki, Y. Inaguma, M. Itoh, and H. Koinuma, J. Appl. Phys. **88**, 3756 (2000).

¹¹C. Ang, A. S. Bhalla, and L. E. Cross, Phys. Rev. B **64**, 184104 (2001).

¹²G. Geneste, J.-M. Kiat, C. Malibert, and J. Chaigneau, Phys. Rev.

B **75**, 174107 (2007).

¹³W. Kohn and L. J. Sham, Phys. Rev. **140**, A1133 (1965).

¹⁴J. P. Perdew and Y. Wang, Phys. Rev. B **45**, 13244 (1992).

¹⁵The ABINIT code is a common project of the Université Catholique de Louvain, Corning Incorporated, and other contributors (URL <http://www.abinit.org>). See also X. Gonze *et al.*, Comput. Mater. Sci. **25**, 478 (2002).

¹⁶N. Troullier and J. L. Martins, Phys. Rev. B **43**, 1993 (1991); **43**, 8861 (1991).

¹⁷Ph. Ghosez, Ph.D. thesis, Université Catholique de Louvain, Louvain, 1997.

¹⁸N. Sai and D. Vanderbilt, Phys. Rev. B **62**, 13942 (2000).

¹⁹W. Zhong and D. Vanderbilt, Phys. Rev. B **53**, 5047 (1996).

²⁰K. A. Müller and H. Burkard, Phys. Rev. B **19**, 3593 (1979).

²¹I. S. Kim, M. Itoh, and T. Nakamura, J. Solid State Chem. **101**, 77 (1992).

²²E. Cockayne and B. P. Burton, Phys. Rev. B **62**, 3735 (2000).

²³D. J. Singh, Phys. Rev. B **53**, 176 (1996).

²⁴A. R. Akbarzadeh, L. Bellaïche, K. Leung, J. Íñiguez, and D. Vanderbilt, Phys. Rev. B **70**, 054103 (2004).

²⁵A. Kokalj, Comput. Mater. Sci. **28**, 155 (2003). Code available from <http://www.xcrysden.org/>